Conformational Analyses of Native and Permethylated Disaccharides

Sanford Mendonca,[†] Glenn P. Johnson,[‡] Alfred D. French,*[,‡] and Roger A. Laine[†,§]

Department of Chemistry, Louisiana State University, Baton Rouge, Louisiana 70803, Southern Regional Research Center, Agricultural Research Service, U.S. Department of Agriculture, 1100 Robert E. Lee Boulevard, New Orleans, Louisiana 70124, and Department of Biological Sciences, Louisiana State University, Baton Rouge, Louisiana 70803

Received: August 25, 2001; In Final Form: January 29, 2002

Effects of permethylation on disaccharide conformation were studied with relaxed-residue ϕ,ψ maps for eight disaccharides of glucose and their permethylated derivatives. Many orientations of the methyl groups were generated with the conformation generator in the Chem-X software program and filtered with a rules-based method. For native molecules, clockwise and counterclockwise rings of hydrogen bonds were also used. MM3(96) energies were calculated with a dielectric constant (ϵ) of 1.5. The native disaccharide maps were also calculated at $\epsilon = 3.5$ and 7.5 to reduce hydrogen-bonding strength. Maps for native and permethylated structures were generally similar. The permethylated structures, which do not make hydrogen bonds, gave maps that were most similar to the native maps that had reduced hydrogen-bonding strength. All ϕ,ψ values for the global minima of the permethylated models fell within the 1-kcal/mol contours on the $\epsilon = 7.5$ maps. Flexibility values based on a partition function were substantially less for permethylated α,α-trehalose and laminarabiose, compared to their native counterparts at any ϵ. On the other hand, strong interresidue hydrogen bonding at $\epsilon = 1.5$ for the global minimum structures of cellobiose and maltose caused those models to be more rigid than their permethylated counterparts. All permethylated models were less flexible than their native counterparts at $\epsilon = 7.5$ and their backbone analogues based on tetrahydropyran calculated at $\epsilon = 1.5$.

Introduction

Methylated carbohydrates are used in both industry and research. In industry, partial methylation is used to alter the properties of native polysaccharides, for example, to make them more soluble in water.[1] In the laboratory, permethylation is a key step in the classic method for determining the chemical sequences of polysaccharides. In the search for bio-based materials, polysaccharide derivatives are of continuing interest. Recently, 2-D NMR analyses were used to characterize 2,3,6-tri-*O*-methyl cellulose to better understand the effects of methylation[2] and derivatization in general.

Another reason for permethylating carbohydrates in the laboratory is that they are more tractable than native sugars when determining structural details by mass spectrometry. The initial impetus for the present conformational analyses was to test a hypothesis that the propensity for molecular fragmentation in mass spectrometers depends on the inverse of the molecular flexibility.[3,4,5] Elsewhere,[6] we have described the results of experimental electrospray collision-induced dissociation (CID) studies of peralkylated disaccharides, accompanied by adaptations of conformational analyses that appear to be useful for discriminating among anomeric configurations.

The same calculations, along with analyses of the native disaccharides, also allow us to investigate how permethylation changes conformational behavior. The purpose of this paper is to discuss the changes in predicted conformation that result from permethylation of eight two-bond-linked, glucose−glucose disaccharides: α,α-trehalose, β,β-trehalose, kojibiose, nigerose, maltose, sophorose, laminarabiose, and cellobiose. α,β-Trehalose was excluded because it is obscure and its linkage is similar to that of sucrose[7] so its MM3 models might be less useful.

Knowledge of the ideal shapes and variability of native and permethylated disaccharides is fundamental to understanding related larger molecules. We are not aware of existing theoretical work on permethylated disaccharides. An MM2 study of the dimeric residue of acetate dipropionate cellulose was reported several years ago.[8]

The main task in this work is to learn the relative influence of increased steric bulk and of eliminated intramolecular hydrogen bonding, both of which are consequences of permethylation. Hydrogen bonds occur often in both experimental crystal structures and computer models of native disaccharides. If native disaccharides were being studied in the mass spectrometer, intramolecular hydrogen bonds would probably also be present. Therefore, energy surfaces for both the permethylated and native disaccharides were calculated with a dielectric constant (ϵ) of 1.5, the value designated for the vacuum phase for the force field that we used.

Comparisons of our previous models with experimentally determined carbohydrate crystal structures indicate that, given our methodology, it is useful to reduce the strength of hydrogen bonding.[9] Therefore, ϕ,ψ energy surfaces were also made for the native disaccharides at $\epsilon = 3.5$ and 7.5. Other than hydrogen bonding, the electrostatic effects in our models of disaccharides are minor, so maps for the permethylated structures were not calculated at higher ϵ. These new analyses of the native disaccharides were not expected to differ much from our previous work.[9,10,11,12] However, several small improvements

* To whom correspondence should be addressed. E-mail: afrench@srrc.ars.usda.gov. Telephone: 504 286-4410. Fax: 504 286-4217.
[†] Department of Chemistry, Louisiana State University.
[‡] U.S. Department of Agriculture.
[§] Department of Biological Sciences, Louisiana State University.

10.1021/jp013290u CCC: $22.00
Published on Web 03/26/2002

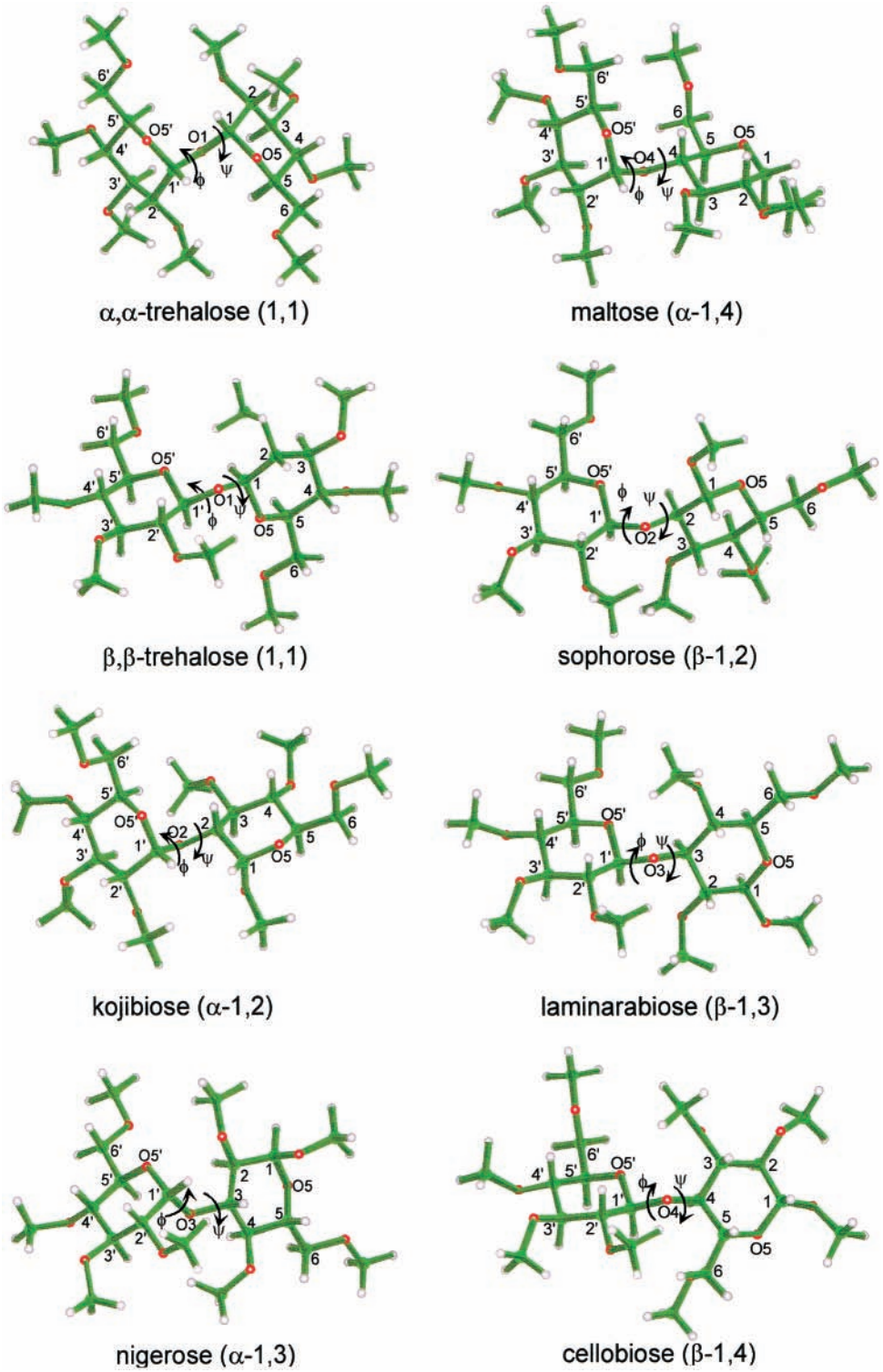

Figure 1. The structures of the permethylated disaccharides at the global minimum in MM3 energy, calculated at $\epsilon = 1.5$. Each molecule is labeled. The carbon atoms are numbered and the ring and glycosidic oxygen atoms are also indicated.

were used in the work on the permethylated disaccharides, so we made new maps for the native molecules, too.

Methods

General. Computerized molecular modeling of disaccharides has been recently reviewed,[13] and our specific strategies are detailed in ref 9. The most important variables of disaccharide conformations are the extents of rotation of the monomeric residues about their bonds to the glycosidic oxygen atom, as indicated by the values of torsion angles ϕ and ψ, shown in Figure 1. The torsion angle for rotation about the glycosidic C-1′—O-*n* bond is denoted by ϕ, and that for rotation about the O-*n*—C-*n* bond to the aglycon is denoted by ψ. For example, the torsion angles for maltose and cellobiose are defined as ϕ = O-5′—C-1′—O-4—C-4 and ψ = C-1′—O-4—C-4—C-5. The use of the non-hydrogen atoms in the definitions was one of the small improvements[9] compared to our earlier work. The energy for each ϕ,ψ combination is plotted on a grid of ϕ and ψ that is often called a Ramachandran map.[14] Such maps are intended to show the lowest energies when ϕ,ψ combinations

are most likely. These energies can be calculated in various ways. Currently, empirical force fields with energy minimization are widely used for disaccharide analysis. A number of such molecular mechanics force fields were recently compared.[15,16] We used the potential energies calculated by the molecular mechanics program MM3(96) that was developed by Allinger et al.[17,18]

MM3 has been used previously with apparent success for many disaccharides. As in other studies, we have used the 1992 parameters for hydrogen bonding. The strengths of the hydrogen bonds in MM3 models depend on the reciprocal of ϵ, and the net enthalpies of a hydrogen bond in a methanol dimer would be about 5.3, 2.27, and 1.05 kcal/mol at ϵ values of 1.5, 3.5, and 7.5, respectively. The MM3(99) O—C—O—H torsion parameters replaced the values of 0.0 distributed with the 1996 and earlier versions of MM3.

Block-diagonal minimization was applied with the default convergence values of 3.6 and 5.52 cal/mol for the native and permethylated sugars, respectively, at 20° intervals of ϕ and ψ. At each interval, all geometric variables were relaxed except ϕ and ψ. The maps show the lowest energy calculated after consideration of all starting models (see below) at each ϕ,ψ point. The axes were shifted so that the maps are visually similar to our earlier maps that were based on torsion angles defined by the glycosidic and aglycon hydrogen atoms in ϕ-H and ψ-H space from −180° to +180°. The tabulated energies for the minima are calculated using a full-matrix minimization method and have values on average 0.46 kcal/mol lower ($\sigma = 0.25$ kcal/mol) than the interpolated map energies at the same values of ϕ and ψ. In a few cases, these isolated structures were higher in energy than indicated by the graphical minima. They were not included in the above average and are indicated in the tables. This accounts for some minor discrepancies between the relative energy minima on the maps and the tabulated energies.

In all, 32 energy surfaces were constructed. They are supplied as Supporting Information. To expedite the comparison of the surfaces for each native and permethylated disaccharide, the maps for the energies computed at $\epsilon = 1.5$ and 7.5 were superimposed on the map for the permethylated molecule. Only the contours at 1, 3, 10, and 20 kcal/mol are shown. A majority of experimental structures should be within the 1-kcal/mol contour, and almost all should be within the 3-kcal/mol contour. The 10- and 20-kcal/mol contours enable comparisons of the surfaces at greater extents of distortion.

Starting Models. Our maps are intended to show the lowest energy possible for the molecule at each ϕ,ψ point. Therefore, all other structural variables must be in states that give the lowest total energy. By itself, however, energy minimization does not ensure that this happens because it finds only the closest local minimum. We attempt to discover the best arrangements of the other structural features by using a substantial number of different "starting models". These structures have different orientations of the individual exocyclic groups; ring shapes other than the observed $^4C_1$ were not considered. If enough starting models are tried, one of them should, when combined with minimization, yield the lowest possible energy at that point.[19]

For the native molecules, known starting structures have rings of intramolecular hydrogen bonds.[20] Those stabilizing rings do not apply to permethylated structures (or disaccharide systems in environments of extremely weak hydrogen bonding).[21] Thus, a challenge of this work was the determination of the likely orientations about the exocyclic bonds to the primary and secondary methoxyl groups. With just three staggered orientations about the 10 bonds, there are $3^{10} = 59\,049$ combinations to consider. That is a larger number of full energy calculations for each ϕ,ψ point than is feasible given our resources. Therefore, we used the following protocol. Initial disaccharides were made by joining glucose rings from the Chem-X[22] fragment library. Reducing ends were given the same configuration as the linkages, that is, the α-anomeric forms for the α-linked reducing disaccharides and β-anomeric forms of the β-linked sugars. Methyl groups were added to the joined fragments. The conformation generator in the Chem-X software program was then used to create combinations of orientations of rotatable groups. Depending on the position in the molecule, there were three, six, or twelve increments of rotation, giving approximately 500 000 000 structures for each permethylated disaccharide. The Chem-X rules-based filter was applied to each. The computer time for filtering is much less than needed to actually calculate energies. It rejects structures that would have high energy, based on internal tables of energies of six-atom sequences. This method made it feasible to systematically scan all structures. Torsion minimization was employed for each selected structure to ensure the viability of the generated conformations. For the permethylated α,α- and β,β-trehaloses, 81 and 243 starting structures were obtained, respectively. The other permethylated disaccharides each yielded 162 starting structures. All starting structures were then minimized with MM3 at each ϕ,ψ point.

Native starting structures were obtained somewhat differently because hydroxyl groups are not covered by the Chem-X rules. The hydroxyl groups on each glucose residue were positioned to make one of three different rings (labeled c, r, or x) that permit intraresidue hydrogen bonds. The c (clockwise) group orientation has its C-1, C-2, C-3, and C-4 hydroxyl groups oriented with torsion angles H—O—C-n—C-(n − 1) = 180°. When $n = 1$, C-(n − 1) becomes O-5. The r (reverse clockwise) orientation has hydroxyl group torsion angles of H—O—C-n—C(n + 1) = 180°. The x combination is the same as r, except H—O—C-2—H = 180°. Thus, nine different combinations, cc, cr, cx, rc, rr, rx, xc, xr, and xx, were made for each disaccharide. For each of these nine different structures, and the initial structure from the Chem-X fragment library, starting structures were then generated using a rules-based search that included only the ϕ and ψ torsion angles and the primary alcohol groups. The increased number of starting models, compared to our previous work, was another of the small improvements mentioned above. The isolated minimum-energy structures were then used for more scans of ϕ,ψ space, increasing the number of unique geometry starting structures.

Flexibility Values. One effect of altered molecular structure would be changes in the calculated molecular flexibility.[23] We define the flexibility over the ϕ,ψ map as the probability volume in degrees squared. The probability is calculated by the Boltzmann relationship, $p_i = e^{-\Delta E/(RT)}$, where ΔE is the potential energy relative to the global minimum, R is the universal gas constant, and T is 298 K. On an energy surface with a 1° grid spacing, the partition function ($\sum p_i$) has essentially the same numerical value as this flexibility. The MM3 energy was interpolated to 1° intervals with the grid function of Surfer 7.0,[24] the program used to calculate the probability volume and produce the contour plots.

A completely flexible molecule would have relative energies of 0.0 kcal everywhere on the ϕ,ψ surface. The value of p_i would therefore be 1.0 at each of the $360 \times 360 = 129\,600$ points. A completely rigid molecule would have $p_i = 1.0$ at one point and a value of 0.0 at all others. Thus, the maximum and minimum possible flexibility values would be 129 600 and 1.0.

TABLE 1: MM3 Energy Minima of Permethylated Disaccharides ($\epsilon = 1.5$)

disaccharide (permethylated)	steric energy[a] (kcal/mol)	relative energy (kcal/mol)	ϕ (deg)	ψ (deg)	glycosidic angle (deg)	location on map
α,α-trehalose	42.09	0.00	79.3	79.3	113.3	
β,β-trehalose	44.05	0.00	−80.1	−80.1	113.0	
		5.36	65.8	−76.1	119.6	
		5.36	−76.1	65.8	119.6	
		9.47	48.6	48.6	125.1	
kojibiose	43.41	0.00	74.9	−160.4	115.0	
		2.10	105.0	−73.1	116.9	
		4.08	85.9	−279.2	121.0	bottom
nigerose	43.95	0.00	101.8	169.3	116.5	
		0.48	75.7	100.4	113.7	
		5.88	101.8	−49.7	120.8	bottom
maltose	44.07	0.00	68.0	−166.7	117.5	
		1.57	108.7	−103.8	116.2	
		1.78	94.6	−287.3	119.2	bottom
sophorose	44.65	0.00	−75.4	−95.7	114.0	
		0.52	−100.1	−168.6	116.2	
		2.22	−67.5	−272.3	120.6	bottom
		5.31	55.2	−118.2	118.4	side
laminarabiose	43.36	0.00	−78.6	142.7	113.6	
		3.59	−132.9	88.1	114.7	
		4.54	−79.7	−59.1	121.5	bottom
		5.92	−279.0	163.8	124.0	side
cellobiose	44.80	0.00	−76.7	−111.6	113.7	
		0.41	−103.0	−165.3	116.3	
		1.12	−83.4	−296.5	120.5	bottom
		4.84	54.6	−117.2	118.3	side

[a] The final steric energy values are those reported by MM3. They are given to allow confirmation of the work during repetition but should not be used to compare different molecules (MM3 calculated heats of formation may be used for that purpose).

Flexibility values were also calculated with MM3 for molecules that consist of two tetrahydropyran rings that had the same linkage configurations as the disaccharides.[23] MM3 maps for these THP−O−THP disaccharide analogues are not shown.

Results and Discussion

Overall Results. *Permethylated Starting Structures*. All of the different molecules had similar starting structures so we use permethylated maltose as an example. During sketching, Chem-X had automatically placed all methyl groups either (+) or (−) gauche to the methine hydrogens. The methyl groups at the C6 positions are trans to C-5. The O-6 is trans to the ring oxygen and gauche to C-4 (the "forbidden"[25] *tg* conformation). After all of the generated structures were subjected to the rules-based filtering, they retained many of these characteristics. The O−Me groups on C-1 of the reducing residues and on C-2 or C-3 of both residues either eclipse or are gauche ($< \pm 60°$) to the respective methine hydrogens. On the nonreducing ring, the O−Me group on C-4′ has varying positions for the different starting structures.

Tvaroska and Carver carried out several applicable ab initio quantum mechanics studies of axial and equatorial 2-methoxylated tetrahydropyrans. Conformations with the methyl group on C-1 (carbohydrate nomenclature) gauche to the ring oxygen were preferred over those having trans positions, because of the exoanomeric effect.[26] In another study,[27] methylation of an added hydroxymethyl group oxygen resulted in the *tg* conformer being slightly favored. Some of our permethylated starting structures also have O-6 in a *tg* conformation. Tvaroska and Carver also studied the rotamer distribution in *O*-methylated axial and equatorial 2,3-, 2,4-, and 2,5-dimethoxy tetrahydropyrans (1,2, 1,3, and 1,4 in carbohydrate nomenclature).[28] The 2,4 and 2,5 models had their lowest energy minima when the methyl groups were either (+) or (−) gauche to the methine hydrogen atoms, again agreeing with our starting models. Crystal structures of permethylated *scyllo*- and *epi*-inositol show that all methoxy carbon atoms have conformations that are close to eclipsing the methine hydrogen atoms.[29,30] These agreements with crystal structures and quantum mechanics results suggest that our starting structures are reasonable.

Minimum Energy Structures of Permethylated Disaccharides. Our MM3 global minimum structures of the permethylated disaccharides are shown in Figure 1, and ϕ,ψ values for all minimum energy permethylated structures are in Table 1. All of them have absolute values of H−C−O−Me torsion angles for the secondary methoxyl groups between 8° and 44°. The primary alcohol chains (Me−O-6−C-6−C-5) on both residues have trans conformations (about 180°). The O6 atoms are either both *gt* or both *gg*.[25] Glycosidic bond angles for the global minimum permethylated structures are approximately the same in all α-linked reducing sugars (kojibiose, nigerose, and maltose) at 115°−117° and in the β-linked sugars (sophorose, laminarabiose, and cellobiose) at 114°. Permethylated α,α- and β,β-trehalose have smaller glycosidic angles of 113.0° and 113.3°, respectively. The glycosidic angles for the permethylated sugars are very similar to the corresponding values for the native disaccharides (Tables 2−4), suggesting that there is no particular interresidue strain associated with permethylation.

Overall Characteristics of the Energy Surfaces. Figures 2 and 3 show the superimposed energy maps and Tables 2−4 contain the data on the minima for the native disaccharides. The individual maps are in Figures 1S−8S of the Supporting Information. The "final steric energy" values for the disaccharides (Tables 2−4) increase as ϵ increases. This is a consequence of the decreased stabilization from the intra- and interresidue

TABLE 2: MM3 Energy Minima of α,α- and *β*,*β*-Trehalose

disaccharide	dielectric constant	steric energy[a] (kcal/mol)	relative energy (kcal/mol)	ϕ (deg)	ψ (deg)	glycosidic angle (deg)
α,α-trehalose	1.5	9.04	0.00	77.8	77.8	113.2
	3.5	17.93[b]	0.00	73.0	77.5	113.2
	7.5	19.78[b]	0.00	78.0	79.0	113.2
β,*β*-trehalose	1.5	10.32[b]	0.00	−78.6	−77.7	113.1
			0.56	−164.4	−85.3	115.4
			0.56	−85.3	−164.4	115.4
			1.98	64.0	−117.6	117.9
			1.98	−117.6	64.0	117.9
			2.48	−79.3	55.6	117.3
			2.48	55.6	−79.3	117.3
			4.49	72.7	72.7	123.9
	3.5	16.48	0.00	−80.7	−80.7	112.9
			3.77	58.7	−79.1	118.3
			3.77	−79.1	58.7	118.3
			5.77	72.8	72.8	124.5
	7.5	19.13	0.00	−80.0	−80.0	113.1
			3.66	−80.9	60.7	118.9
			3.66	60.7	−80.9	118.9
			6.64	72.8	72.8	124.7

[a] The final steric energy values are those reported by MM3. They are given to allow confirmation of the work during repetition but should not be used to compare different molecules (MM3 calculated heats of formation may be used for that purpose). [b] Our automated procedure for isolating minima does not find more than one minimum within a 20° grid square. There should be a symmetry-related minimum having interchanged ϕ and ψ values.

TABLE 3: MM3 Energy Minima of Kojibiose, Nigerose, and Maltose

disaccharide	dielectric constant	steric energy[a] (kcal/mol)	relative energy (kcal/mol)	ϕ (deg)	ψ (deg)	glycosidic angle (deg)	location on map
kojibiose	1.5	9.53	0.00	89.3	−77.7	116.6	
			1.04	76.9	−136.5	112.8	
			2.09	110.8	58.0	119.7	top
			3.70	176.1	−55.2	120.4	NE[b]
	3.5	18.07	0.00	87.4	−76.3	116.5	
			0.03	81.0	−161.9	114.7	
			3.23	95.5	−293.9	120.0	bottom
	7.5	19.85	0.00	78.0	−161.7	114.7	
			0.49	89.9	−77.1	116.7	
			3.15	90.4	−292.2	120.3	bottom
nigerose	1.5	9.47	0.00	92.0	154.2	115.6	
			0.17	109.5	98.0	114.2	
			2.28	89.1	−49.8	118.9	bottom
			4.07	183.0	180.9	119.5	NE[b]
	3.5	18.07	0.00	90.9	161.5	115.9	
			1.26	87.9	107.3	113.7	
			2.74	93.6	−50.8	119.1	bottom
	7.5	20.34	0.00	92.1	162.0	116.2	
			0.66	82.8	102.6	113.8	
			2.13	95.6	−51.6	119.2	bottom
maltose	1.5	9.12	0.00	108.4	−145.5	114.3	
			2.94	88.2	−281.6	118.3	bottom
			7.99[c]	56.4	−197.6	119.8	
	3.5	19.54	0.00	94.5	−148.2	113.4	
			1.17	91.1	−284.3	118.7	bottom
			2.25[d]	110.9	−110.1	115.8	central
	7.5	21.23	0.00	96.7	−146.3	114.2	
			0.89	93.5	−286.0	118.6	bottom

[a] The final steric energy values are those reported by MM3. They allow confirmation of the work during repetition but should not normally be used to compare different molecules (MM3 calculated heats of formation may be used for that purpose). Because all of the group enthalpy corrections are the same for the molecules in this table, however, the final steric energies are comparable. [b] Nonexoanomeric. [c] This full-matrix minimized structure was 2.00 kcal/mol higher in energy than predicted from the Surfer grid. [d] This full-matrix minimized structure was 0.57 kcal/mol higher in energy than predicted from the Surfer grid.

hydrogen bonds. Final energies for the permethylated structures (Table 1) are also higher because of their additional atoms.

Maps for the trehaloses are symmetrical about the $\phi = \psi$ diagonal because of inherent molecular symmetry. They also differ from the maps for the reducing molecules because the latter typically have some elongation of the 1-kcal/mol contours

TABLE 4: MM3 Energy Minima of Sophorose, Laminarabiose, and Cellobiose

disaccharide	dielectric constant	steric energy[a] (kcal/mol)	relative energy (kcal/mol)	ϕ (deg)	ψ (deg)	glycosidic angle (deg)	location on map
sophorose	1.5	9.69	0.00	−109.8	−95.9	114.0	
			0.28	−293.9	−113.8	117.9	side
			0.29	−85.0	−175.6	115.5	central
			0.81	−142.2	−132.5	113.9	central
			2.46	−86.3	41.7	118.7	top
			3.02	−186.7	−176.8	118.5	NE[b]
	3.5	17.63	0.00	−91.3	−176.1	116.1	
			0.52	−89.2	48.6	118.6	top
			0.76	−78.8	−97.8	113.8	central
			1.19	−297.1	−113.4	118.5	side
	7.5	19.57	0.00	−93.5	−171.1	116.2	
			0.31	−80.8	−105.7	113.7	
			1.02	−90.0	51.3	118.7	top
			2.70	−298.9	−114.7	118.5	side
laminarabiose	1.5	8.87	0.00	−88.8	81.1	115.8	
			2.24	−294.6	127.6	118.8	side
			2.70	−87.9	283.8	118.7	top
			6.05	−184.1	64.6	119.9	NE[b]
	3.5	16.62	0.00	−91.2	84.7	116.0	
			0.38	−79.5	142.3	113.5	
			3.09	−90.2	287.2	118.7	top
			4.45	−297.8	130.2	119.0	side
	7.5	18.85	0.00	−79.9	143.0	113.7	
			0.78[c]	−92.5	80.2	116.3	
			2.22	−90.7	287.7	118.7	top
			4.12	−299.6	130.4	118.8	side
cellobiose	1.5	7.72	0.00	−87.9	−142.0	115.3	
			0.70	−294.1	−122.4	117.9	side
			3.43	−91.0	51.7	118.3	top
			6.33	−46.2	−65.7	120.1	central
	3.5	17.60	0.00	−91.8	−163.3	116.1	
			0.59	−77.8	−128.0	114.3	
			1.44	−88.7	54.3	118.7	top
			1.75	−295.5	−122.4	118.7	side
	7.5	19.50	0.00	−76.0	−119.7	113.9	
			0.21	−94.1	−159.4	116.4	
			1.72	−89.7	56.6	119.0	top
			3.50	−299.9	−123.1	118.6	side

[a] The final steric energy values are those reported by MM3. They allow confirmation of the work during repetition but should not normally be used to compare different molecules (MM3 calculated heats of formation may be used for that purpose). Because all of the group enthalpy corrections are the same for the molecules in this table, however, the final steric energies are comparable. [b] Nonexoanomeric. [c] This full-matrix minimized structure was 0.18 kcal/mol higher in energy than predicted from the Surfer grid.

in the ψ direction. This is due to the fairly deep well resulting from the exoanomeric effect, compared to the flatter well for the aglycon torsion.

Kojibiose, nigerose, and maltose have their lowest energy regions in similar troughs with $\phi \approx 100°$. The maximum barriers to complete rotation about the aglycon bond are 6−8 kcal/mol. Rotation about the glycosidic bond is more difficult because barriers are 11−19 kcal/mol. The diequatorial disaccharides, sophorose, laminarabiose, and cellobiose, have ψ-rotations that are similar to those of the axial−equatorial sugars, except that the path is in the position appropriate for the changed configuration with $\phi \approx -100°$. Also, some barriers are as low as 3 kcal/mol. These linkages allow less-inhibited ϕ-rotation compared to axial−equatorial linkages, with barriers of 7−10 kcal/mol.

All global minima are consistent with the exoanomeric effect. Thus, O-5′—C-1′—O-*n*—C-*n* torsion angles are ±68−110°, positive for α- and negative for β-linkages. Further, their H—C-1′—O-*n*—C-*n* torsion angles (ϕ-H) are between ±10° and ±53°, negative for α- and positive for β-linkages. All reducing native and permethylated models have secondary minima in the neighborhood of $\phi = \pm 80°$ and $\psi = -300°$ or +60° (−60° or +300° for nigerose and laminarabiose). These secondary minima, which also conform to the exoanomeric effect, are described as near the top or bottom of the maps. Secondary minima at the bottom (and top) edges are fairly interesting for permethylated sophorose (2.2 kcal/mol) and maltose (1.8 kcal/mol) and especially interesting for permethylated cellobiose (1.1 kcal/mol).

The β-linked sophorose, laminarabiose, and cellobiose models give additional secondary minima on the sides of the maps at roughly $\phi = -300°$ or +60°. They are also are stabilized by the exoanomeric effect because they too have aglycon carbons gauche to O-5′, but C-*n* is also placed gauche to C-2′. This placement gauche to two large atoms increases the potential energy. That strain is indicated (Tables 1 and 4) by the substantially larger glycosidic angles for all minima located near the sides of the energy maps. Similar strain results from placement of the glycosidic carbon atom between two carbon atoms for conformations at the tops or bottoms of the maps for all of the reducing disaccharides (see also Table 3). The diequatorial native structures at $\epsilon = 1.5$ with side-of-the-map conformations are stabilized by two interring hydrogen bonds. Their energies of 0.28, 2.24, and 0.70 kcal/mol (Table 4) indicate

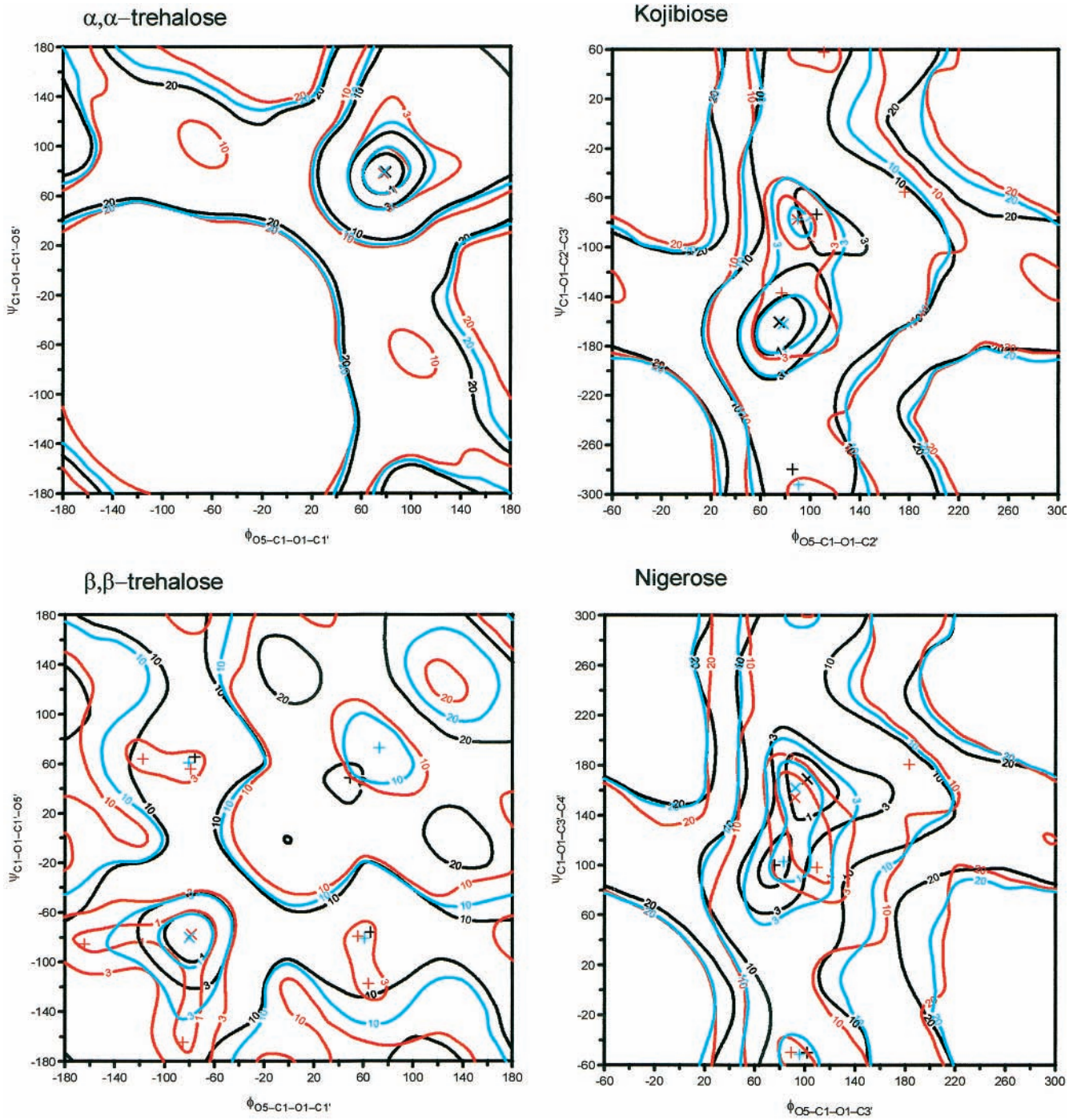

Figure 2. The superimposed MM3 energy surfaces for α,α-trehalose, *β*,*β*-trehalose, kojibiose, nigerose, and their permethylated counterparts. The name of the disaccharide is above each of the plots. The black lines correspond to the permethylated molecules (at $\epsilon = 1.5$), the red to the $\epsilon = 1.5$ surfaces for the native molecules, and the blue to the $\epsilon = 7.5$ surfaces for the native molecules. Contours are shown for 1, 3, 10, and 20 kcal/mol. The original individual surfaces are in Supporting Information, Figures 1S−4S. The isolated global minima are indicated by ×, and the + signs indicate secondary minima, colored like the contour lines.

that the hydrogen bonds have nearly overcome the additional steric strain. These minima are all much less important on the permethylated maps, with energies >4.8 kcal/mol.

Four minima that have relatively high energies have ϕ values of about 180° and thus are not stabilized by the exoanomeric effect. These nonconforming minima for native kojibiose, nigerose, sophorose, and laminarabiose were only isolated on the $\epsilon = 1.5$ maps, indicating stabilization by strong hydrogen bonds. Two secondary minima for sophorose and permethylated laminarabiose were intermediate relative to either the exoanomeric effect or a staggered conformation, with ϕ values of −142.2° and −132.9°, respectively.

Flexibility Values. Flexibility values, including those for the THP−O−THP disaccharide analogue molecules, are shown in Table 5. Overall, methylated molecules are less flexible than their corresponding native disaccharides at $\epsilon = 7.5$ or their corresponding THP−O−THP analogues. The large value for *β*,*β*-trehalose at $\epsilon = 1.5$ is discussed below. Values for α,α-trehalose indicate little flexibility, apparently because of its diaxial linkage and dual exoanomeric effects. However, maltose

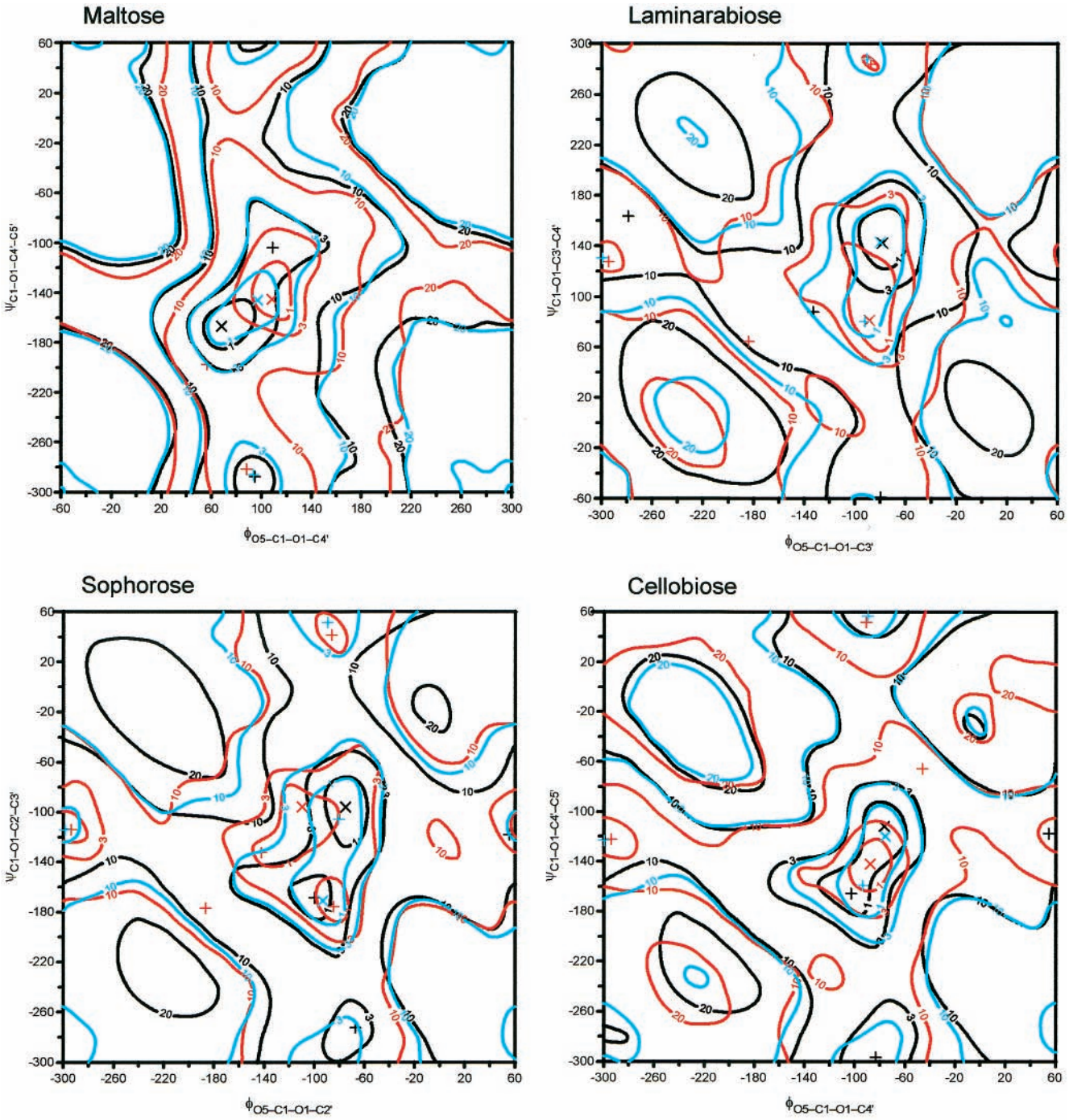

Figure 3. The superimposed MM3 energy surfaces for maltose, sophorose, laminarabiose, cellobiose, and their permethylated counterparts. The name of the disaccharide is above each of the plots. The black lines correspond to the permethylated molecules (at $\epsilon = 1.5$), the red to the $\epsilon = 1.5$ surfaces for the native molecules, and the blue to the $\epsilon = 7.5$ surfaces for the native molecules. Contours are shown for 1, 3, 10, and 20 kcal/mol. The original individual surfaces are in Supporting Information, Figures 5S−8S. The isolated global minima are indicated by ×, and the + signs indicate the secondary minima, colored like the contour lines.

and cellobiose also have very low flexibility values at $\epsilon = 1.5$, apparently because of strong interresidue hydrogen bonding. At the higher ϵ values, the relative rigidity of α,α-trehalose is retained, but the flexibility values of cellobiose and maltose increase substantially. At the higher ϵ values, the diequatorial disaccharides, sophorose, laminarabiose, and cellobiose, are the most flexible, but at $\epsilon = 1.5$, various forces are counterbalanced and no trend is visible. Flexibility values for the permethylated 1,3-linked disaccharides are fairly different from the 1,2- and 1,4-linked molecules, an observation for which we have no explanation.

Comparisons of the Individual Permethylated and Native Disaccharides. α,α-*Trehalose.* The MM3 maps of native and permethylated α,α-trehalose (Figures 2 and 1S) are very similar to each other. Of all of these models, α,α-trehalose is the most sterically restricted, as indicated by the low flexibility values in Table 5 and the large areas above 20 kcal/mol on its maps. The flexibility values and the areas above 20 kcal/mol are very different indicators of steric hindrance. The flexibility values represent normal conformational variation, whereas structures with energies over 20 kcal/mol are quite strained. The ϕ and ψ values for the minimum energy conformations for all α,α-

TABLE 5: Molecular Flexibility Values Based on a 1° Interval Partition Function (See Methods)

		native disaccharide dielectric constant			
disaccharide	THP−O−THP[a]	1.5	3.5	7.5	methylated
α,α-trehalose	701	635	751	616	470
β,β-trehalose	749	1773	948	850	715
kojibiose	1707	786	1230	1180	851
nigerose	1467	1338	958	1355	1281
maltose	1451	688	1267	1305	820
sophorose	1708	2051	2253	2396	1382
laminarabiose	1581	1455	1902	1867	832
cellobiose	1960	665	1447	1701	1605

[a] Values for the laminarabiose and cellobiose molecules are smaller than the MM3 values in ref 22. Quantum mechanical HF/6-31G* flexibility values for the analogues in that work are somewhat higher, in general.

trehalose models are nearly identical (Tables 1 and 2). Thus, permethylation does not induce a conformational change but does reduce the flexibility. We confirmed the slightly asymmetric values for the $\epsilon = 3.5$ global minimum by starting the minimization from a symmetric structure with ϕ and $\psi = 72.5°$. There is no interresidue hydrogen bonding at or near the global minimum, leaving the MM3 maps fairly insensitive to changes in ϵ or permethylation.

β,β-Trehalose. The β,β-trehalose maps (Figures 2 and 2S) are similar to each other. However, the unusual shape of the 1-kcal/mol contour for the native disaccharide at $\epsilon = 1.5$ is not found for the permethylated structure. The predicted flexibility of β,β-trehalose at $\epsilon = 1.5$ (Table 5) is higher than that of the THP−O−THP model as well as higher than all but one of the other disaccharides at that ϵ. This is due to the O-2—O-5′ hydrogen bonds that stabilize the secondary minima at −85°, −164° and −164°,−85°. Although interatomic H···O distances are greater than 3.0 Å at the global minimum in energy, small torsion angle changes in either the negative ϕ or ψ directions away from the global minimum reduce one of the two O-2—O-5′ distances. Thus, the resulting decrease in exoanomeric stabilization is mostly offset by the increasing strength of the hydrogen bond. That gives an extended 1-kcal/mol contour. The secondary minima on the $\epsilon = 1.5$ surface at $\phi = 64°$, $\psi = -118°$ and $\phi = -118°$, $\psi = 64°$ are much lower than the corresponding minima on the permethylated map. On the native maps, these minima are stabilized by O-2—O-2′ hydrogen bonds. Another secondary native minimum at about $\phi = 72°$, $\psi = 72°$ has an energy of 4.5 kcal/mol on the $\epsilon = 1.5$ surface. The intrinsic strain is indicated by its very high glycosidic angle. The energy is much lower than its counterparts on the permethylated map or on the maps for the native molecule at $\epsilon = 3.5$ or 7.5. Thus, permethylation also diminishes the importance of the secondary minima, with the overall effect being similar to increasing the ϵ values.

Kojibiose. The maps for kojibiose (Figures 2 and 3S) all show two central minima. When hydrogen bonding is impossible, as with the permethylated molecule, or weakened, when $\epsilon = 7.5$, the minimum near $\psi = -160°$ is preferred. When hydrogen bonding is stronger, with $\epsilon = 1.5$ or 3.5, the minimum near $\psi = -80°$ is favored, stabilized by a strong hydrogen bond between O-3 and O-5′. At $\epsilon = 3.5$, O-6′ is also an acceptor from O-3 but the two central minima are almost equienergetic. The $\psi = -162°$ structure can form a very weak hydrogen bond between O-2′ and O-1. This liaison was found for the secondary $\epsilon = 3.5$ structure but not for the $\epsilon = 7.5$ global minimum. Thus, the permethylation of kojibiose favors a conformation that, when taken by the native molecule, is not dependent on hydrogen bonding for stabilization.

Nigerose. All global minima on the nigerose maps (Figures 2 and 4S, Table 3) are very close. The native global minima all have O-2—O-5′ hydrogen bonds. A weak O-4—O-2′ link is also found for the $\epsilon = 1.5$ map. At the minimum on the $\epsilon = 1.5$ map, O-6′ is *tg*, but for the minima at higher ϵ, O-6′ is *gt* and it shares the proton donated by O-2. The secondary native central minima are stabilized by O-4—O-2′ hydrogen bonds.

The secondary minimum that is counter to the exoanomeric effect has an energy of 4.07 kcal/mol on the $\epsilon = 1.5$ map (Table 3). That region becomes a plateau on the $\epsilon = 3.5$ and 7.5 native and permethylated maps. It is stabilized by a strong O-2—O-2′ hydrogen bond. The native structures at the secondary, bottom minima all have (stronger) O-4—O-6′ and (weaker) O-4—O-5′ bifurcated hydrogen bonds and weak O-2—O-2′ interactions, but the bottom permethylated conformation is similar.

Maltose. The maltose maps in Figures 3 and 5S have two or three minima. The secondary central minima on the $\epsilon = 1.5$ and 3.5 surfaces were separated from the global minima by very low energy barriers, as well as having higher energies than indicated by the maps (Table 3). The global minima for the native molecules are all near $\phi,\psi = 100°,-145°$ and are stabilized by O-3—O-2′ interresidue hydrogen bonds. The $\epsilon = 3.5$ minimum also has an O-6—O-6′ interaction. The global minimum for the permethylated structure is at $\phi = 68°$, $\psi = -166°$. That conformation corresponds to more than 4.0 kcal/mol on the $\epsilon = 1.5$ surface for the native disaccharide, but is well inside the extended 1.0-kcal/mol contour on the $\epsilon = 7.5$ map. The conformation of the permethylated molecule, if applied to the native disaccharide, does not allow interresidue hydrogen bonding, but it is stabilized better by the exoanomeric effect than are the global minimum native structures that are stabilized more by hydrogen bonding. So, the fairly large shift in ϕ,ψ values can again be explained by the inability of the permethylated structure to form hydrogen bonds. The native bottom minima are all stabilized by O-3—O-6′ and O-5′ bifurcated hydrogen bonds, and the $\epsilon = 1.5$ structure also has a strong O-2′—O-6 hydrogen bond. However, the ϕ,ψ values of the comparable permethylated structure are nearly identical.

Sophorose. The central regions on all sophorose surfaces (Figures 3 and 6S) have two nearly equal minima. A third minimum, at 0.81 kcal on the $\epsilon = 1.5$ surface with $\phi = -142.2°$, is inside the same 1-kcal/mol contour as the global minimum. It results from a strong O-2′—O-3 hydrogen bond but is not stabilized by either the exoanomeric effect or a fully staggered linkage conformation and is absent from the other surfaces. The upper minima are favored on the $\epsilon = 1.5$ native and permethylated maps. However, their ϕ values differ by nearly 35°. On the $\epsilon = 3.5$ and 7.5 maps, the lower ψ values are preferred. The global minimum on the $\epsilon = 1.5$ surface has a strong O-3—O-2′ hydrogen bond, while the $\epsilon = 3.5$ and 7.5 global minima have only very weak O-1—O-6′ linkages. The central secondary minimum structure ($\phi = -78.8°$, $\psi = -97.8°$) on the $\epsilon = 3.5$ surface that best corresponds to the global minimum on the $\epsilon = 1.5$ surface has no interresidue hydrogen bonds, while the similar structure on the $\epsilon = 7.5$ map has the same O-3—O-2′ hydrogen bond found for the $\epsilon = 1.5$ surface. The nonexoanomeric minimum on the $\epsilon = 1.5$ map ($\phi = -186.7°$) is stabilized by an O-1—O-2′ hydrogen bond. The relative energy of that conformation is similar on the other maps, but it is no longer a minimum.

All top or bottom secondary minima also have low energy, ranging from 0.52 to 1.02 kcal/mol on the native maps. For a

somewhat shifted minimum on the permethylated map, the energy is 2.22 kcal/mol. The side minima have low energies on the native maps (0.28, 1.19, and 2.70 kcal/mol as ϵ increases). The secondary minima near the edges all have O-3—O-5′ hydrogen bonds, and ones from the tops of the $\epsilon = 1.5$ and 3.5 maps are bifurcated with O-6′ as the secondary acceptor. The ones on the sides also have O-2′—O-1 linkages.

Laminarabiose. The 3- and 10-kcal/mol contours for the permethylated and $\epsilon = 7.5$ native laminarabiose maps differ more than for the other disaccharides (Figures 3 and 7S). The 3-kcal/mol contour on the $\epsilon = 7.5$ map touches the 10-kcal/mol contour on the permethylated map at the point $\phi = -60°$, $\psi = 60°$ (Figure 3). Steric effects are also indicated by the reduced flexibility for the permethylated structures compared to the native $\epsilon = 7.5$ structures (Table 5). Still, the global minimum on the permethylated map falls almost exactly on its counterpart on the $\epsilon = 7.5$ map.

All native, global-minimum structures are stabilized by an O-4—O-5′ hydrogen bond, with O-4 also donating to O-6′ at $\epsilon = 1.5$ and 3.5. The O-4—O-5′ bond is quite weak for the $\epsilon = 7.5$ global minimum and the corresponding secondary minimum on the $\epsilon = 3.5$ map. Structures of the native secondary minima on the edges all have O-4—O-2′ and O-2—O-5′ hydrogen bonds. The structure that corresponds to the nonexoanomeric minimum on the $\epsilon = 1.5$ map was not a minimum at higher dielectric constants but retained the high relative energy.

Cellobiose. All surfaces for cellobiose (Figures 3 and 8S) are similar. The correspondence between the 3- and 10-kcal/mol contours on the 7.5 and permethylated maps is only closer for α,α-trehalose. The global minimum on the permethylated surface is very near the global minimum on the $\epsilon = 7.5$ disaccharide surface. A unique high-energy minimum was found on the $\epsilon = 1.5$ map, with $\phi = -46.2°$, $\psi = -65.7°$, stabilized by a O-6′—O-6 hydrogen bond. No minimum was isolated from the plateau (Figure 8S, $\epsilon = 1.5$) for the nonexoanomeric conformation at $\phi = -180°$, $\psi = -180°$.

All global minima for native cellobiose have O-3—O-5′ hydrogen bonds, the only interring hydrogen bond at $\epsilon = 7.5$. The $\epsilon = 1.5$ global minimum structure has another, O-6—H···O-2′. The $\epsilon = 3.5$ minimum has a bifurcated interaction of O-3 with O-6′. The two secondary minima on the edges differ in importance, depending on the model. The minimum at the side has lower relative energy on the $\epsilon = 1.5$ surface, while the minima at the top or bottom are favored at the higher ϵ values and for the permethylated structure. The native structures on all edges have O-6—O-6′ hydrogen bonds, with O-2—O-5′ hydrogen bonds for the side structures as well.

Conclusions

MM3 was used to generate relaxed residue ϕ,ψ maps for eight two-bond-linked glucose−glucose disaccharides and their permethylated derivatives. Generally, the permethylated molecules gave maps similar to those of the native disaccharides, especially those computed at $\epsilon = 7.5$, in which hydrogen bonds give minimal stabilization. The global minima for permethylated structures fell within the 1-kcal/mol contours on the respective $\epsilon = 7.5$ native maps. This explains why conformations of crystal structures of disaccharides and their derivatives are often similar.

Values of the glycosidic bond angles were very comparable for the native and permethylated structures, suggesting that there is little strain across the linkage added by permethylation, at least at the minima. However, flexibility values were reduced for permethylated molecules compared to the native molecules at $\epsilon = 7.5$ as well as to the simple backbone molecules based on tetrahydropyran. We conclude that, while there is a modest steric effect from permethylation, larger effects arise from the variation in treatment of hydrogen bonding in the model. Differences in the exact response to permethylation depend on the complex interplay of the different contributions to the potential energy. Predicting these detailed responses requires case-by-case examinations.

Supporting Information Available: The individual energy surfaces for the native disaccharides at ϵ values of 1.5, 3.5, and 7.5 and for the permethylated molecules (Figures 1S−8S). This material is available free of charge via the Internet at http://pubs.acs.org.

References and Notes

(1) Majewicz, T. G.; Podlas, T. J. In *Kirk−Othmer Encyclopedia of Chemical Technology*, 4th ed.; Kroschwitz, J. I., Ed.; Wiley, New York, 1993; Vol. 5, p 541.

(2) Sachinvala, N. D.; Hamed, O. A.; Winsor, D. L.; Niemczura, W. P.; Maskos, K.; Parikh, D. V.; Glasser, W.; Becker, U.; Blanchard, E. J.; Bertoniere, N. R. *J. Polym. Sci., Part A: Polym. Chem.* **1999**, *37*, 4019.

(3) Laine, R. A.; Pamidimukkala, K. M.; French, A. D.; Hall, R. W.; Abbas, S. A.; Jain, R. K.; Matta, K. L. *J. Am. Chem. Soc.* **1988**, *110*, 6931.

(4) Laine, R. A.; Yoon, E.; Mahier, T. J.; Abbas, S.; deLappe, B.; Jain, R.; Matta, K. *Biol. Mass Spectrom.* **1991**, *20*, 505.

(5) Yoon, E.; Laine, R. A. *Biol. Mass Spectrom.* **1992**, *21*, 479.

(6) Mendonca, S.; Cole, R. B.; French, A. D.; Johnson, G. P.; Zhu, J.; Cai, Y.; Laine, R. A. *J. Am. Soc. Mass Spectrom.*, submitted for publication.

(7) French, A. D.; Kelterer, A. M.; Cramer, C.; Johnson, G. P.; Dowd, M. *Carbohydr. Res.* **2000**, *326*, 305.

(8) Iwata, T.; Okamura, K.; Azuma, J.; Tanaka, F. *Cellulose* **1996**, *3*, 107−124.

(9) French, A. D.; Kelterer, A.-M.; Johnson, G. P.; Dowd, M. K.; Cramer, C. J. *J. Mol. Graphics and Modell.* **2000**, *18*, 95.

(10) Dowd, M. K.; Reilly, P. J.; French, A. D. *J. Comput. Chem.* **1992**, *13*, 102.

(11) Dowd, M. K.; Zeng, J.; French, A. D.; Reilly, P. J. *Carbohydr. Res.* **1993**, *230*, 223.

(12) Dowd, M. K.; French, A. D.; Reilly, P. J. *Carbohydr. Res.* **1992**, *233*, 15.

(13) Von der Lieth, C. W.; Kozar, T.; Hull, W. E. *J. Mol. Struct. (THEOCHEM)* **1997**, *395*, 225.

(14) Sasisekharaan, V. Stereochemical Criteria for Polypepetides and Proteins. *Collagen; proceedings of a symposium sponsored by the Central Leather Research Institute, Council of Scientific and Industrial Research, Madras, India, and held at the Institute on November 29-30, 1960*; Interscience Publishers: New York, 1962; Vol. 1060, pp 39−78. Rao, V. S. R.; Sundarajan, P. R.; Ramakrishnan, C.; Ramachandran, G. N. *Conformation in Biopolymer*; Academic Press: London, 1963.

(15) Gundertofte, K.; Palm, J.; Pettersson, I.; Stamvik, A. *J. Comput. Chem.* **1991**, 12.

(16) Perez, S.; Imberty, A.; Engelson, S. B.; Gruza, J.; Mazeau, K.; Barbero, J. J.; Poveda, A.; Espinoza, J. F.; Eyck, V. B.; Johnson, G.; French, A. D.; Kouwijzer, M. L.; Grootenhuis, P.; Bernadi, A.; Raimondi, L.; Senderowitz, A.; Durier, V.; Vergoten, G.; Rasmussen, K. *Carbohydr. Res.* **1998**, *314*, 141.

(17) Allinger, N. L.; Rahman, M.; Lii, J. H. *J. Am. Chem. Soc.* **1990**, *112*, 8293.

(18) MM3 is available to academic users from the Quantum Chemistry Program Exchange, Creative arts, Indiana University, Bloomington, IN. Commercial users may obtain MM3 from Tripos Associates, St. Louis, MO.

(19) French, A. D.; Brady, J. W. *ACS Symp. Ser.* **1990**, *430*, 1.

(20) French, A. D.; Tran, V. H.; Perez, S. *ACS Symp. Ser.* **1990**, *430*, 191.

(21) Stortz, C. *Carbohydr. Res.* **1999**, *322*, 77.

(22) Chem-X is no longer distributed by Oxford Molecular, a subsidiary of Pharmacopeia.

(23) French, A. D.; Kelterer, A.-M.; Johnson, G. P.; Dowd, M. K.; Cramer, C. J. *J. Comput. Chem.* **2001**, *22*, 65.

(24) Surfer is available from Golden Software, Golden, CO.

(25) Marchessault, R. H.; Perez, S. *Biopolymers* **1979**, *18*, 2639.

(26) Tvaroska, I.; Carver, J. P. *Carbohydr. Res.* **1998**, *309*, 1.

(27) Tvaroska, I.; Carver, J. P. *J. Phys. Chem. B* **1997**, *101*, 2992.

(28) Tvaroska, I.; Carver, J. P. *J. Mol. Struct. (THEOCHEM)* **1997**, *395*, 1.

(29) Anderson, J. E.; Angyal, S. J.; Craig, D. C. *J. Chem. Soc., Perkin Trans. 2* **1997**, *729*.

(30) Anderson, J. E.; Angyal, S. J.; Craig, D. C. *Carbohydr. Res.* **1995**, *272*, 141.